Flow Research Report No. 449

MODEL TESTS TO COMPARE CAPSIZE RESISTANCE OF THE USCG 44' MLB AND PROPOSED 47' MLB IN BREAKING WAVES

John J. Zseleczky
Louise A. Wallendorf
Jim H. Duncan

December 1987

APPROVED FOR PUBLIC RELEASE
DISTRIBUTION UNLIMITED

FLOW RESEARCH, INC.
21414 - 68th Avenue South
Kent, Washington 98032
(206) 872-8500

UNCLASSIFIED

SECURITY CLASSIFICATION OF THIS PAGE (When Data Entered)

REPORT DOCUMENTATION PAGE	READ INSTRUCTIONS BEFORE COMPLETING FORM
1. REPORT NUMBER	2. GOVT ACCESSION NO. AD-A197420 / 3. RECIPIENT'S CATALOG NUMBER
4. TITLE (and Subtitle) Model Tests to Compare Capsize Resistance of the USCG 44' MLB and Proposed 47' MLB in Breaking Waves	5. TYPE OF REPORT & PERIOD COVERED: Final 6. PERFORMING ORG. REPORT NUMBER: Flow Res. Report No. 449
7. AUTHOR(s) John J. Zseleczky, Louise A. Wallendorf, James H. Duncan	8. CONTRACT OR GRANT NUMBER(s): N00014-84-C0698
9. PERFORMING ORGANIZATION NAME AND ADDRESS: Flow Research, Inc., 21414-68th Avenue South, Kent, WA 98032	10. PROGRAM ELEMENT, PROJECT, TASK AREA & WORK UNIT NUMBERS
11. CONTROLLING OFFICE NAME AND ADDRESS	12. REPORT DATE: December 1987 13. NUMBER OF PAGES: 33
14. MONITORING AGENCY NAME & ADDRESS(if different from Controlling Office)	15. SECURITY CLASS. (of this report): UNCLASSIFIED 15a. DECLASSIFICATION/DOWNGRADING SCHEDULE
16. DISTRIBUTION STATEMENT (of this Report): Unlimited	
17. DISTRIBUTION STATEMENT (of the abstract entered in Block 20, if different from Report)	
18. SUPPLEMENTARY NOTES: Also published by U.S. Naval Academy as Report No. EW-14-87.	
19. KEY WORDS (Continue on reverse side if necessary and identify by block number)	
20. ABSTRACT (Continue on reverse side if necessary and identify by block number): The U.S. Coast Guard has designed a new 47' Motor Lifeboat which has twice the design speed of the existing 44' Motor Lifeboats. Because of the difference in design speeds, the hulls are considerably different. This report documents model tests and techniques used to compare the capsize resistance of the two boats in beam-sea breaking waves. The new 47' Motor Lifeboat was found to be less prone to capsize than the older 44' Motor Lifeboat.	

DD FORM 1 JAN 73 1473 EDITION OF 1 NOV 65 IS OBSOLETE

S/N 0102-LF-014-6601

UNCLASSIFIED

SECURITY CLASSIFICATION OF THIS PAGE (When Data Entered)

TABLE OF CONTENTS

LIST OF TABLES

LIST OF FIGURES

Nomenclature

B	Maximum beam of boat	(ft)
C_W	Wave celerity	(ft/sec)
Disp	Hull Displacement (weight)	(lb)
f	Wave frequency	(hz)
GM_T	Transverse metacentric height of hull	(ft)
g	Acceleration caused by gravity	(ft/sec^2)
H	Wave height	(ft)
H_0	Deep water wave height	(ft)
KG	Height of hull center of gravity above keel	(ft)
k_{xx}	Hull radius of gyration in roll	(ft)
L	Length of wave; also length of boat (LBP)	(ft)
L_0	Deep water wave length	(ft)
LBP	Length between perpendiculars	(ft)
LCG	Longitudinal center of gravity; measured forward of aft perpendicular	(ft)
MLB	Motor Lifeboat	
s_C'	Crest front steepness *	
T	Period of wave; also roll period of boat	(sec)
V	Velocity	(ft/sec)
μ_H	Horizontal asymmetry *	
μ_V	Vertical asymmetry *	
ν	Kinematic viscosity of water	(ft^2/sec)
ρ	Mass density of water	($lb\text{-}sec^2/ft^4$)
σ	Surface tension of water	(lb/ft)

* See Figure 3.

1.0 Introduction

Coast Guard rescue boats frequently operate in surf zones near beaches, areas of strong currents with waves at the mouths of rivers, and in rough seas caused by high winds. During these operations they are subjected to the risk of capsizing due to encounters with breaking waves. At the present time, there is no established method for designing capsize resistant boats. Theoretical efforts to attack this problem are hindered by the complexity of capsize events. The first major difficulty is the flow field. The approach of the wave to the breaking event is a highly nonlinear, unsteady, free surface flow. In the process of breaking itself the flow also becomes turbulent and entrains air. Potential flow numerical techniques have been used to follow the flow field up to breaking, but little or no work has been done to describe the ensuing turbulent flow. The next major difficulty is the description of the response of the boat to the flow field. Its motion is highly dependent on the position of the boat relative to the breaking event. The resulting motion is, of course, not describable by linear theory.

In view of the complexity of the phenomenon, the most fruitful approach to determining the capsize resistance of an existing vessel is to develop a laboratory testing capability. The first step in the development of this capability is choosing the waves. Waves break in nature due to shoaling, interaction with a current field (at an inlet or the mouth of a river), or wave-wave interactions in the open ocean. In the present study we have generated breaking waves by a wave-wave interaction technique in which a train of waves of varying frequency is used. Due to the dispersive characteristics of the waves, the wave train converges as it moves along the tank, eventually forming a breaker. Work of this type was begun at the United States Naval Academy in 1982 [1,2]. This technique was later modified so that a given breaker type, ranging from a spilling to a plunging breaker, could be produced at various wave frequencies [3]. Having chosen the waves, one must next choose the method of testing the model with the waves. Of particular importance is the position and orientation of the model relative to the breaking wave. Boats are probably most vulnerable to breakers in a beam sea orientation resulting from loss of power or broaching in following seas. With this in mind, both the earlier work [1,2] and the present work have used the beam sea orientation. During the earlier tests, a single breaking wave was produced and used to capsize the model. The position of the model relative to the breaker and a number of dynamic and geometric characteristics of the model were varied in an attempt to change its capsizing resistance. The study showed that

position and roll moment of inertia had significant effects on whether a boat would capsize when struck by a breaking wave.

In the present experiments we have recognized that, for a given model, there will always be breaking waves large enough to cause capsizing and waves small enough so that the model will resist capsizing. Increasing the capsize resistance of a design will mean increasing the maximum wave size for which it remains upright. With this fact in mind, two wave forms, one a strong plunging breaker and one a spilling breaker, were scaled to a number of wave heights and lengths. Two 1/16th scale models - one of the existing 44' Motor Lifeboat (44 MLB) and the other of the proposed 47' Motor Lifeboat (47 MLB) - were tested for capsize resistance with the waves.

The remainder of the report is divided into four sections. In section 2 the experimental apparatus and techniques are discussed. In section 3, the results of the capsizing tests are presented and discussed. The results include maximum roll angle versus position for each wave and model, and a qualitative description of the motion of the model relative to the wave during the encounter. The relationship of the test data to full scale performance is discussed in section 4 and estimates of the relative probability of capsize for the two designs are given. Finally, the conclusions of the study are presented in section 5.

2.0 Experimental Details

2.1 Tanks

The model tests were carried out in two wave tanks at the United States Naval Academy Hydromechanics Laboratory. Most of the tests were run in the smaller of the two tanks, which is 120 feet long, 8 feet wide and 5 feet deep. A wavemaker is located at one end of the tank and consists of two horizontally hinged flaps which are sealed at the tank walls (see Figure 1 for details). A hydraulic actuator is used to drive the lower board with respect to the tank foundation; a second actuator drives the upper wave board with respect to the lower wave board. Tests with a larger wave were conducted in the Laboratory's 380 foot long tank. This tank is 26 feet wide and 16 feet deep as shown in Figure 2. The wavemaker is a larger version of the system used in the 120 foot long tank.

2.2 Waves

A series of geometrically scaled breaking waves were developed using the Hydromechanics Laboratory's computer program which drives the wavemaker to produce a series of waves of increasing amplitude and period which converge to form a breaking wave at a repeatable location in the wave tank [3,4]. The plunging and spilling breakers previously developed and described in [3] were not severe enough to capsize either the 44 MLB or the 47 MLB, so a large plunging breaker was developed which would capsize both vessels. This plunging breaker was scaled down to four smaller plunging breakers; five spilling breakers were created from the plunging breaker drive signals by adjusting the peak signal phase and overall signal amplitude. The wavemaker drive signal parameters for these waves are summarized in Table I. A detailed description of the drive signal is described in [3].

The breaking wave profiles were measured near the breakpoint and characterized by single probe measurements. The probe location was set according to the criteria established in [3], at the point where the height of the crest reached a maximum value; this point was close to the point where the wave visually appeared to break. Water surface profile measurements were taken with MTS variable resistance wave probes at a sampling frequency of 500 hertz, using a Hewlett Packard engineering workstation with a 12 bit analog to digital converter. The wave signal was filtered with a 20 hertz Ithaco analog low pass filter. The wave signal was truncated to include the preceding trough, crest and following trough of the breakers shown in

Figure 3. Wave asymmetry parameters, crest front steepness (s_c'), asymmetry about a horizontal axis (μ_H), and asymmetry about a vertical axis (μ_V) were calculated from the water surface profile at the breakpoint. A thorough discussion of the evolution of these wave asymmetry parameters during the breaking process is described in [3]. The average values of the asymmetry parameters at the breakpoint for the spilling and plunging breakers in the present experiments are given in Table II.

In the discussion of test results the different plunging and spilling breakers are referred to in terms of their breaking wave periods rather than wave heights. Figure 3 shows how breaking wave period (T_d) is defined using a fixed wave probe time history of wave height. The wave periods of the plunging breakers used in the test program ranged from 3.3 seconds to 7.2 seconds (full scale). The spilling breaker wave periods ranged from 4.8 seconds to 7.6 seconds. Two different measures of breaking wave height are included in Table I for each wave: crest height measured above mean still water, and crest-to-trough height. As can be seen in the table, crest height always increases with increasing wave period, but crest-to-trough height does not always increase. Therefore, the wave with the longest period and largest crest height does not necessarily have the largest crest-to-trough height. When observing the waves in the laboratory, the waves with longer periods were clearly more powerful than the shorter period waves. Therefore, each wave is referred to in terms of wave period rather than wave height throughout this report.

2.3 Models

One-sixteenth scale models of the 44 MLB and the proposed 47 MLB were used in the test program. The 44 MLB model was built from a commercially available fiberglass shell which was modified at the Naval Academy to conform with the lines shown in Coast Guard Drawing 44MLB(S)0500-2 RE10. The 47 MLB model was built out of high density, closed cell foam and fiberglass. The 47 MLB model hull conforms to an unnumbered Coast Guard lines drawing dated 29 May 86, by D. Ghosh. The superstructure was modeled according to Coast Guard Drawing 47MLB 802-7,8 and 11, Rev. A.

Since projected side area and realistic 360 degree roll righting characteristics were considered to be essential in these experiments, the key elements of each hull's superstructure were built into the models as listed:

44 MLB

1) Forward deckhouse with raised console
2) Wrap around windshield
3) Aft deckhouse
4) Cockpit well
5) Radar

47 MLB

1) Deckhouse with flying bridge and side bulkheads
2) Side hull cut outs
3) Aft lazarette
4) Flying bridge seat lockers
5) Radar enclosure

Figures 4 and 5 show outboard profiles and body plans for the two boats.

Each model was ballasted with the center of gravity located as specified by the Coast Guard; Table III shows the values used for longitudinal center of gravity (LCG) and vertical center of gravity (KG). Roll inertia for the full scale hulls was an unknown, so estimates were made based on the limited information available. Reference [6] suggests the following relationship between roll inertia and beam for surface ships:

$$1.108k_{xx} = 0.44B \quad , \text{ or}$$

$$k_{xx}/B = 0.397 \quad ,$$

where:

k_{xx} = roll radius of gyration

B = beam of ship

There were problems in ballasting the models with both the specified centers of gravity and the estimated roll inertia. In order to obtain the low center of gravity specified for the 47 MLB model, all of the moveable ballast was placed as low as possible. The resulting k_{xx}/B was 3 percent below the suggested value of 0.397. The 44 MLB model was easily ballasted to the specified center of gravity, but the highest obtainable k_{xx}/B was 12 percent below the suggested value. Table III shows the final values used. It was suspected that the relatively tall superstructure of the 47 MLB was responsible for the model's higher k_{xx}/B. If that were the case, the difference in k_{xx}/B for the two models may be more representative of the boats in full scale than if the models were arbitrarily set up with equal values of k_{xx}/B. No attempt was made to model

pitch gyradius. The test program involved the beam sea condition in which roll angles were typically ten times greater than pitch angles, so the effect of pitch gyradius should not be significant.

The hydrostatic righting characteristics of the two models were physically measured in the tank at heel angles of zero through 180 degrees. The measurements have been expanded to full scale and are presented in Figure 6. Details and discussion of the model righting arm experiments are documented in [7].

2.4 Procedures

Although little work has been done to investigate the effects of model scale ratios on capsize testing in breaking waves, three well established physical relationships are generally thought to be of importance:

Froude Number	$[C_w/(gL)^{0.5}]$model = $[C_w/(gL)^{0.5}]$ship
Reynolds Number	$[C_wL/\nu]$model = $[C_wL/\nu]$ship
Weber Number	$[\sigma/(g\rho L^2)]$model = $[\sigma/(g\rho L^2)]$ship

Since the forward speed of the boat in these tests is zero, boat speed cannot be used to determine Froude or Reynolds Numbers. Instead, wave speed and wave length are used. It is impossible to model all three Numbers at once so a compromise must be made, keeping in mind the implications of the compromise when analyzing the test results. Since capsizing is clearly dominated by wave action, there is little doubt that Froude Number - the parameter which determines proper scaling of waves, gravity and inertia effects - is the most important relationship to scale. If the correct Froude Number is used, the Reynolds Number for the model is too low and the Weber Number is too high. The low Reynolds Number may slightly increase the model damping due to skin friction relative to full scale. The high model Weber Number may alter the characteristics of the the wave jet that strikes the hull. Since these scale effects have not been quantified we cannot say how accurately Froude scaled capsize tests simulate full scale events. We should however be able to reduce the risk of making poor full scale predictions if we limit ourselves to comparing the two models in terms of relative capsize resistance rather than absolute capsize resistance.

The overall test plan was to compare the motion of the two models in a family of breaking waves at different positions with respect to the oncoming breaker. The worst case scenario was assumed to be with the boat at zero speed,

broadside to a breaking wave; this was the only condition studied. Ideally the two hulls would have been tested simultaneously, at the same position in the same wave, but this was not practical because of physical limitations. Instead, a repetitive test sequence was set up in which one model was tested immediately after the other. A timed interval of 3 minutes between tests was chosen to ensure that background disturbances from previous tests had dissipated.

Repeatable model positions were made possible using the model release mechanism shown in Figure 7, which was based on a method described in [8]. Each model was outfitted with eyelets made of 1/8 inch diameter wire, located at the bow and stern, at the height of the center of gravity (near the nominal roll axis). Rods 1/2 inch in diameter were lowered through the eyelets from a beam mounted on the model towing carriage. The rods were simultaneously raised out of the eyebolts when the mechanism was triggered by a signal from the wavemaking computer. With this system both models were "launched" identically, several wave periods before the breaking event. Tests were run with the model released at several locations before and after the breakpoint of the wave. The release location was varied by moving the model towing carriage to different locations along the length of the tank.

For an estimation of relative behavior in breaking waves, the peak roll angle caused by the wave impact was measured for each condition. This roll angle will be referred to as the "impact roll angle" throughout the discussion. In some cases this was not the maximum roll angle, as will be explained later, but it provided a consistent reference point. The harsh realities of ballasting these small models with realistic mass distributions eliminated the possibility of on board sensors and telemetry gear. Instead, a simple method was used for measuring roll angle with a video camera, stop-action recorder, and protractor on the monitor screen. Checks were made to quantify camera parallax error by statically restraining the models at various known angles and displacements with respect to the camera. The maximum parallax error (which occured only under extreme conditions) was found to be +/-5 degrees. Impact roll angles measured by a given observer were found to be repeatable within +/-10 degrees. Different observers typically measured angles on the high or low side. A brief analysis of measurements made by different observers showed that 75 percent of measurements were within 11 degrees and 90 percent were within 17 degrees. The considerable difference between measurements of different observers was caused by the haziness of the model's television image as it moved sideways under the spray of the wave. Although each observer interpreted the image somewhat differently, there

was reasonable repeatability for a given observer. In order to minimize the scatter in the recorded results, the measurements of one observer were used exclusively, except in cases where the differences between observers was extreme. For these cases, the video's were carefully reviewed and discussed to find the reason for the discrepancy. Then the impact roll angles were re-measured by the original observer.

3.0 Results and Discussion

Before discussing details of the test results, some terminology will be established. Consider a stationary boat model floating in the tank with its longitudinal axis perpendicular to the longitudinal axis of the tank. The following terms will be used to describe the motions of that boat in beam sea breaking waves:

Upstream	- Toward the wavemaker
Downstream	- Away from the wavemaker
Upstream roll	- Roll in which deckhouse moves toward the wavemaker more than keel
Downstream roll	- Roll in which deckhouse moves away from the wavemaker more than keel
Impact roll angle	- Peak downstream roll angle caused by wave crest striking hull
Wave Breakpoint	- Longitudinal position in tank where breaking wave crest curls over and touches preceding trough

In a typical test run, the model started to roll with the slope of the waves preceding the breaker. Upon impact, the model rolled violently downstream under the force of the jet of water in the breaking wave crest. In certain positions with respect to the wave breakpoint, the wave jet landed on the upstream deck in such a way that the jet impulse opposed the roll motion induced by the waveslope. Here, the maximum roll angle was not the impact roll angle measured immediately after wave impact, but instead, the angle induced by the waveslope before or after the breaker. For these cases, the angle recorded was the smaller angle - the impact roll angle.

Figure 8 shows the impact roll angle for each boat at various positions upstream and downstream of the wave breakpoint, for the five plunging breakers used in the test program. The response of the 44 MLB is on top, in Figure 8a and the response of the 47 MLB is below. The distance between the position in which the model was released and the breakpoint is represented on the horizontal axis of the plots. This position has been nondimensionalized by the average beam of the two boats which is 13 feet in full scale. In the plots, a "Distance from Breakpoint / Beam" of +2.0 represents a test where the model was released two beams downstream of the point where the wave broke. Negative positions, on the far left of the plots represent cases where the models were released well upstream of the wave breakpoint. At these positions the models rode over the rising, but not yet breaking wave crest. Positive positions, at the far right represent cases where the models were released downstream of the breaker and were only mildly

tossed around in the turbulent aftermath of the breaker. The two models were knocked down or capsized only when they were within a zone of about plus or minus four beams from the breakpoint. In this zone, the 44 MLB capsized in the three longer period waves of the five plunging waves tested, whereas the 47 MLB capsized in only one - the longest period wave.

Although the 47 MLB capsized far less often than the 44 MLB, there were several cases in the shorter period breakers where the 47 MLB rolled to higher angles for a given wave and position. These results were cross-plotted to allow a comparison of the two boats in waves of different periods. In Figure 9, the ranges of position down the tank for which each hull rolled to a given angle are plotted as a function of wave period. Range of position is nondimensionalized by beam and the wave period is plotted in the dimensionless form: $[(g*T^2)/B]^{0.5}$. The plots show that the 47 MLB rolled more than the 44 MLB in the less powerful, short period waves while the 44 MLB rolled more in the stronger, long period waves. Also, the 44 MLB capsized over a much wider range of positions than the 47 MLB.

Some specific observations from the video tapes of the plunging wave tests help explain the humps and hollows in the maximum roll angle data shown in Figure 8. The dramatic decrease in roll angle, which consistently occurred when the model was released around the breakpoint, was found to be caused by the force of the wavejet when it crashed down on the upstream deck. This situation only occurred over a narrow range of positions. When the models were released upstream of this zone, the wavejet struck the exposed freeboard and augmented the waveslope induced roll. The 47 MLB model had more freeboard and therefore more lateral area exposed to the wave jet in this zone. It is important to realize however, that the wave jet never impacted broadside on the large 47 MLB superstructure; the hull always rose up with the soon-to-be-breaking wave crest and took the blow on the side of the hull. When the model was released downstream of the breakpoint, the wavejet freely crashed into the preceding wave trough, causing what resembled an underwater explosion. The upwelling of water from the impact pushed up against the bottom of the hull. The boat's upstream side was closer to the impact so it experienced higher pressures than the downstream side, resulting in a rolling moment in the same direction as the roll induced by the wave slope. Again, the 47 MLB had more exposed bottom area than the 44 MLB so it rolled more at this position.

Careful observations were made of the videotapes for cases where the 44 MLB capsized and the 47 MLB resisted. At the instant of wave impact, both hulls were rolled away from the wave, at approximately the same angle. Within 0.5

seconds, model scale (2 seconds full scale), both hulls were rolled past 90 degrees. The 47 MLB hesitated and resisted rolling past about 100 degrees while the 44 MLB kept on rolling. The hydrostatic curves of Figure 6 show that the 47 MLB has significantly greater righting moment past 90 degrees than the 44 MLB. Other factors such as inertia and center of gravity may contribute to the difference in capsize resistance, but the 47 MLB's hesitation around 100 degrees appears to be directly attributable to the hull's greater righting moment.

Neither boat capsized in the spilling breakers made in the 120 foot tank (Figure 10) or in the extreme spiller made in the 380 foot tank (Figure 11). The test results were plotted in the same manner used for the plunging breakers, but an expanded roll angle scale was used. The 44 MLB roll angles are shown at the top of Figure 10 and the 47 MLB data are below. The maximum roll angle of the 44 MLB was consistently greater than for the 47 MLB at all positions with respect to the breakpoint. As each model was released farther downwind, the maximum roll angle of both boats decreased. Apparently, the energy that dissipated as the wave spilled reduced the impact experienced by the models.

The models were also tested in regular, sinusoidal waves of constant height and varying frequency to find the period of roll resonance. Figure 12 shows the results from these tests. In 2.7 foot high beam sea waves, the 44 MLB rolled 35 degrees at its resonant point and the 47 MLB rolled 25 degrees at its resonant point. The wave periods where roll resonance occured were around 3.7 seconds for the 44 MLB and around 3.0 seconds for the 47 MLB (full scale). The formula used to predict still water roll period is: $\text{Period} = 1.108k_{xx} / (GM_T^{0.5})$ [6]. This is based on simple harmonic motion for small roll angles, with no damping. The formula predicts natural roll periods of 3.7 seconds for the 44 MLB and 2.7 seconds for the 47 MLB. It is interesting to see that the zero-damping formula closely predicts the true roll period of the 44 MLB but under-predicts the period of the 47 MLB. The hard chines of the 47 MLB presumably provide more roll damping than the round bottom of the 44 MLB. This would give the hull a longer roll period than the "no-damping" formula predicts.

The wave periods of the plunging breakers used in the test program were between 3.3 and 7.2 seconds (full scale), with the 7.2 second wave being the most powerful plunger. From the breaking wave tests it was found that both boats capsized in the 7.2 second breaker and neither capsized in the 3.3 second breaker. This shows that the resonant roll period in regular waves should not be used to predict the breaking wave period that will capsize a boat. The main reason for this is that as breaking wave period increases, wave height, wave speed and the amount of energy carried in

the wave increase. Ignoring the absolute differences, the regular wave resonant period may be useful for predicting relative performance in breaking waves. The test results show that the 47 MLB rolled more than the 44 MLB in the short period waves and less than the 44 MLB in the long period waves; this would have been predicted by looking at the regular wave data alone.

4.0 Relationship of Laboratory Results to Field Conditions

In this section, we attempt to use the laboratory data comparing the roll angles of the two models in the presence of deepwater breaking waves to make an estimate of the relative roll and capsize resistance of the two designs in the field. Rather than a detailed prediction of full scale performance at a given test site, the following is a rough estimate using our limited laboratory data, first order methods to predict the breaker characteristics in the field, and simple methods to scale the laboratory waves to those found in the field. At this point in the development of the testing technique, more detailed predictions of full-scale performance are not warranted.

The most practical cases of boats capsizing in breaking waves for the U.S. Coast Guard probably occur as waves propagate into shallow water. These areas include the shorelines, inlets, and the mouths of rivers. As a deepwater wave propagates into shallow water the period of the wavetrain (T), remains constant while the wavelength (L), height (H), and steepness (H/L) of the wavetrain first decrease slightly and then increase dramatically [9]. In deep water, the wavetrain is close to sinusoidal in shape; however, as it moves into shallow water the crests become narrow and high and the troughs become wide and shallow. At this point, the profile is close to that of a solitary wave. For these waves, the wavelength is effectively infinite and the wave is completely described by its crest to trough height, H. The shoaling wave eventually breaks, and the breaker type, ranging from a spilling to a plunging breaker, is determined by the steepness of the wave in deep water, H_0/L_0. If the deep water steepness is close to its limiting value, the wave will break as soon as it steepens slightly due to shoaling. These waves form spilling breakers. If the deep water wave steepness is very small, it forms a solitary wave and becomes a plunging breaker. In practice, waves with deep water steepness greater than 0.01 form spilling breakers while those with less steepness form plunging breakers (see Reference 9).

Making shoaling breakers for the laboratory tests was impractical because of excessive tank length requirements. In the present laboratory tests, the breakers were produced in deep water by interaction of wave components in a wave train. As it approaches breaking, the wave form steepens, its period decreases and it eventually forms a spilling or a plunging breaker. These waves never evolve into shapes like solitary waves, however breaking waves in deep and shallow water have gross similarities. In order to estimate the behavior of our models in shoaling waves, we compare the deepwater and shoaling breaking waves based on the height from the mean water level to the crest.

As a test site for comparison of the breaker heights and types in the field to those used in the laboratory experiments, we chose the area near the mouth of the Columbia River. This site has the advantage of being the training ground for the USCG Motor Lifeboat School, and of having a NOAA wave data buoy located near by at 46.2 degrees north latitude and 124.2 degrees west longitude. Table IV gives the distribution of wave height and period from this data buoy. Consider first the shoaling of the waves. For a wave shoaling on a shallow sloped beach independent of shoreline shape and currents, we can use standard wave forecasting techniques to predict the height and type of breaking waves. Using the deep water wave data in Table IV and the wave shoaling theory [9] we find the distribution of shoaling wave heights (mean water level to breaking wave crest) to be:

Crest Height Range (feet)	Percent of Wave Heights Within Range	Percent of Wave Heights Exceeding Range
0 - 3.75	17.6	82.4
3.75 - 7.50	39.3	43.1
7.50 - 11.3	32.2	10.9
11.3 - 15.0	5.4	5.5

The breaker heights from the experiments can be expanded to full scale by multiplying the laboratory wave height data in Table I by 16, the prototype to model scale ratio. Using Froude scaling, $T/(gL)^{0.5}$ is held constant, so the full scale wave periods are calculated by multiplying the laboratory data by 4 (the square root of the scale ratio). The following table shows the full scale characteristics of the laboratory waves:

Plunging Breakers		Spilling Breakers	
Period (sec)	Height * (ft)	Period (sec)	Height * (ft)
3.28	8.27	4.80	9.32
5.88	10.0	5.60	7.20
6.40	10.8	7.64	21.30
6.80	12.3		
7.20	12.5		

* Heights measured from mean still water to breaking crest

Comparison of the full scale height of the laboratory waves and the height of waves in the field indicates that there is some overlap. The range of laboratory waves was

chosen so that the smaller amplitude plunging breakers (shorter period) did not capsize the models while the larger amplitude (longer period) waves did. Waves with still larger amplitudes would be even more likely to capsize the models. For the spilling breakers, the laboratory data indicates that the 47 MLB rolls less than the 44 MLB and since waves of these scaled heights occur in the field it appears that this conclusion will be valid at the test site. For the plunging breakers, the range of distances over which either boat capsizes can be combined with the frequency of occurrence of those wave heights in the field to obtain a single plot. Such a plot appears in Figure 13. It shows that waves capable of capsizing either boat exist at the test sight (according to this very rough calculation), but that a smaller percentage of waves are capable of capsizing the 47 MLB.

5.0 Conclusions

With breaking waves on the beam and with zero forward speed, the proposed 47 MLB will be less likely to capsize than the 44 MLB. This appears to be mainly attributable to the reserve buoyancy of the 47 MLB when rolled past 90 degrees. No assessments were made in this test program about either boat's ability to avoid the vulnerable beam sea condition. This is an important point that should be addressed elsewhere. In smaller, shorter period plunging breakers, the 47 MLB will roll to higher maximum angles than the 44 MLB. This has been attributed to the higher beam and corresponding higher GM of the 47 MLB. In longer period plunging and spilling breakers, the 47 MLB will roll less than the 44 MLB.

When exposed to non-breaking beam seas with a dominant period near the boat's natural roll period, the 47 MLB will roll less than the 44 MLB for a given wave height.

References

1. Kirkman, K.l., Nagle, T.J. and Salsich, J.O.; "Sailing Yacht Capsizing", SNAME 6th CSYS, Annapolis, MD, 1983.

2. Salsich, J.O. and Zseleczky, J.J.; "Experimental Studies of Capsizing in Breaking Waves", AIAA/SNAME 13th Ancient Interface Symposium, Vol. 29, San Diego, CA, 1983.

3. Duncan, J.H., Wallendorf, L.A. and Johnson, B.; "An Experimental Investigation of the Kinematics of Breaking Waves", Proceedings IAHR Symposium on Wave Generation in Laboratory Basins, Laussanne, Switzerland, 1987.

4. Salsich, J.O., Johnson, B. and Holton, C.; "A Transient Wave Generation Technique", Proceedings 20th ATTC, Hoboken, NJ, 1983.

5. Myrhaug, D. and Kjeldsen, P.; "Parametric Modelling of Joint Probability Density Distributions for Steepness and Asymmetry in Deep Water Waves", J. Coastal Engineering, Amsterdam, 1983.

6. "Principles of Naval Architecture", SNAME, New York, NY, 1967.

7. Hudgens, J.A.; "Hydrostatic Righting Arm Measurements for Models of the U.S. Coast Guard 44' and 47' Motor Lifeboats", U.S. Naval Academy Hydromechanics Laboratory Technical Note: 87-1, Annapolis, MD, 1987.

8. Claughton, A. and Handley, P.; "An Investigation into the Stability of Sailing Yachts in Large Breaking Waves", Wolfson Unit, University of Southampton, UK, 1984.

9. H.O. Publication No. 234; "Breakers and Surf, Principles of Forcasting", U.S. Naval Oceanographic Office, Washington, D.C., Reprinted 1969.

	Plunging					Spilling		
Wave File	11	17a	18	12	13	21	16	EX
Period (sec)	1.80	1.70	1.60	1.47	0.82	1.4	1.2	1.91
Wavelength (ft)	16.6	14.8	13.1	4.9	3.4	10.0	7.38	18.5
Crest Height (ft)	0.781	0.769	0.675	0.625	0.517	0.450	0.583	1.33
Crest-Trough Height (ft)	0.950	0.967	0.975	0.808	0.750			
f(start) (hz)	1.05	1.10	1.15	1.20	1.37	1.15	1.20	0.795
f(peak) (hz)	0.613	0.641	0.669	0.700	0.800	0.664	0.700	0.464
f(stop) (hz)	0.525	0.550	0.574	0.600	0.686	0.574	0.600	0.397
Theor. Break Pt. (ft)	111	101	92.8	85.0	65.0	92.8	85.0	194
Delay Time (sec)	2.095	1.954	1.739	0.833	1.423	1.608	1.541	
Span Settings								
(Upper)	4.60	4.00	3.70	4.10	2.90	2.60	2.46	1.96
(Lower)	6.90	6.00	5.55	6.15	4.44	3.90	3.70	1.96

Table I - Model Scale Characteristics of Laboratory Waves and Wavemaker Drive Signal Parameters

	Average Asymmetry Parameter		
	$s_{C'}$	μ_H	μ_V
Type of Breaking Wave			
Plunging	0.60	0.79	2.0
Spilling	0.37	0.71	1.7

Table II - Breaking Wave Asymmetry Parameters

	44 MLB		47 MLB	
	Model	Ship	Model	Ship
Length Overall (ft)	2.76	44.1	2.96	47.3
Length Between Perp. (ft)	2.50	40.0	2.69	43.0
Beam, Max. (ft)	0.744*	11.9*	0.875	14.0
Draft, w/o skeg (ft)	0.19	3.0	0.19	3.0
Displacement (lbs)	9.43	38,300	10.1	42,600
LCG, fwd. of AP (ft)	1.26	20.1	1.08	17.2
KG (ft)	0.262	4.19	0.303	4.85
GM_T (ft)	0.100	1.60	0.313	5.00
k_{xx}, roll gyradius (ft)	0.263	4.20	0.338	5.41
LBP/B	3.36		3.07	
$(Disp/2240)/(LBP/100)^3$	267		239	
LCG/LBP	0.503		0.400	
k_{xx}/B	0.354		0.386	

* 44 MLB beam does not include rub rails.

Table III - Hull Characteristics As Tested

PERCENT FREQUENCY OF WAVE HEIGHT (METERS) VS WAVE PERIOD (SECONDS)

WBOUC
DECEMBER, JANUARY, FEBRUARY — LATITUDE 46.2N LONGITUDE 124.2W

WAVE PERIOD (SEC)	DIR	WAVE HEIGHT(METERS) 0.5-1.0	1.5-2.0	2.5-3.0	3.5-4.0	4.5-5.0	5.5-6.0	6.5-7.0	7.5-8.0	8.5-9.0	9.5-10.0	>10	TOT %	TOT N
>15.5	**	.0	.1	.2	1.3	1.1	.7	.4	.1	*	*	.0	4.0	408
11.6-15.5	**	3.2	6.1	14.3	9.2	4.2	2.0	.7	.2	.1	*	.0	42.0	4315
7.6-11.5	**	5.2	17.9	19.5	9.6	3.2	1.0	.3	.1	*	*	.0	56.1	5691
6-7.5	**	.2	1.1	1.0	.2	.1	.0	.0	.0	.0	.0	.0	2.6	263
<6	**	2.0	.6	*	.0	.0	.0	.0	.0	.0	.0	.0	2.7	275
TOT %		10.7	25.7	35.0	19.1	8.3	3.7	1.4	.4	.2	.1	.0	100.0	
TOT N		1087	2605	3543	1939	844	376	142	44	20	7	0		10172

WBOUC
MARCH, APRIL, MAY — LATITUDE 46.2N LONGITUDE 124.2W

WAVE PERIOD (SEC)	DIR	WAVE HEIGHT(METERS) 0.5-1.0	1.5-2.0	2.5-3.0	3.5-4.0	4.5-5.0	5.5-6.0	6.5-7.0	7.5-8.0	8.5-9.0	9.5-10.0	>10	TOT %	TOT N
>15.5	**	.3	.7	1.8	1.4	.2	.2	*	.0	.0	.0	.0	4.6	250
11.6-15.5	**	1.7	6.5	14.6	9.2	2.2	.5	.1	.1	*	*	.0	35.9	1938
7.6-11.5	**	3.9	25.1	15.0	5.9	1.5	.3	.1	*	.0	.0	.0	56.1	3211
6-7.5	**	.0	1.1	.9	.2	.0	.0	.0	.0	.0	.0	.0	4.9	278
<6	**	.5	.2	*	.0	.0	.0	.0	.0	.0	.0	.0	.7	42
TOT %		6.4	33.6	32.3	15.3	3.8	1.0	.2	.1	*	*	.0	100.0	
TOT N		366	1919	1844	731	219	59	17	6	1	1	0		5719

WBOUC
JUNE, JULY, AUG — LATITUDE 46.2N LONGITUDE 124.2W

WAVE PERIOD (SEC)	DIR	WAVE HEIGHT(METERS) 0.5-1.0	1.5-2.0	2.5-3.0	3.5-4.0	4.5-5.0	5.5-6.0	6.5-7.0	7.5-8.0	8.5-9.0	9.5-10.0	>10	TOT %	TOT N
>15.5	**	.0	.0	.0	.0	.0	.0	.0	.0	.0	.0	.0	.0	0
11.6-15.5	**	.1	.4	1.6	.6	.4	.3	.0	.0	.0	.0	.0	3.4	141
7.6-11.5	**	25.0	39.1	5.7	.4	.1	.0	.0	.0	.0	.0	.0	71.4	2916
6-7.5	**	16.9	4.9	.5	*	.0	.0	.0	.0	.0	.0	.0	21.3	870
<6	**	3.1	.7	.0	.0	.0	.0	.0	.0	.0	.0	.0	3.9	159
TOT %	**	44.0	45.0	7.8	.5	.0	.0	.0	.0	.0	.0	.0	100.0	
TOT N	**	1810	1844	319	19	2	0	0	0	0	0	0		4112

WBOUC
SEPTEMBER, OCTOBER, NOVEMBER — LATITUDE 46.2N LONGITUDE 124.2W

WAVE PERIOD (SEC)	DIR	WAVE HEIGHT(METERS) 0.5-1.0	1.5-2.0	2.5-3.0	3.5-4.0	4.5-5.0	5.5-6.0	6.5-7.0	7.5-8.0	8.5-9.0	9.5-10.0	>10	TOT %	TOT N
>15.5	**	.2	.4	.3	.7	.5	.4	.2	.1	*	.0	.0	3.1	318
11.6-15.5	**	2.6	7.4	4.6	6.3	2.2	1.2	.5	.2	.1	*	.0	25.1	2550
7.6-11.5	*	16.2	27.4	12.1	5.4	1.9	.6	.1	.0	.0	.0	.0	63.8	6481
6-7.5	**	2.1	2.9	.4	.2	.0	.0	.0	.0	.0	.0	.0	5.8	593
<6	**	1.6	.4	.0	.0	.0	.0	.0	.0	.0	.0	.0	2.1	217
TOT %	*	21.7	38.4	20.4	12.6	4.7	2.2	.8	.3	.1	*	.0	100.0	
TOT N	1	2207	3736	2116	1277	476	226	79	30	10	1	0		10159

WBOUC
ANN AL — LATITUDE 46.2N LONGITUDE 124.2W

WAVE PERIOD (SEC)	DIR	WAVE HEIGHT(METERS) 0.5-1.0	1.5-2.0	2.5-3.0	3.5-4.0	4.5-5.0	5.5-6.0	6.5-7.0	7.5-8.0	8.5-9.0	9.5-10.0	>10	TOT %	TOT N
>15.5	**	.1	.7	.9	.9	.6	.4	.2	.1	*	*	.0	3.9	1176
11.6-15.5	**	1.9	6.9	10.4	6.2	2.5	1.2	.4	.1	.1	*	.0	29.7	8944
7.6-11.5	*	12.2	27.0	12.6	5.8	2.0	.6	.2	*	*	*	.0	57.4	17319
6-7.5	*	3.0	3.7	.8	.2	.0	.0	.0	.0	.0	.0	.0	6.7	2030
<6	**	1.7	.7	*	.0	.0	.0	.0	.0	.0	.0	.0	2.3	693
TOT %	*	19.0	39.0	24.8	13.0	5.1	2.2	.8	.3	.1	*	.0	100.0	
TOT N	1	5736	13944	7434	3936	1539	661	238	80	31	*	0		30162

Table IV - Columbia River Wave Buoy Data
From: NOAA NDBC Publication April 1986

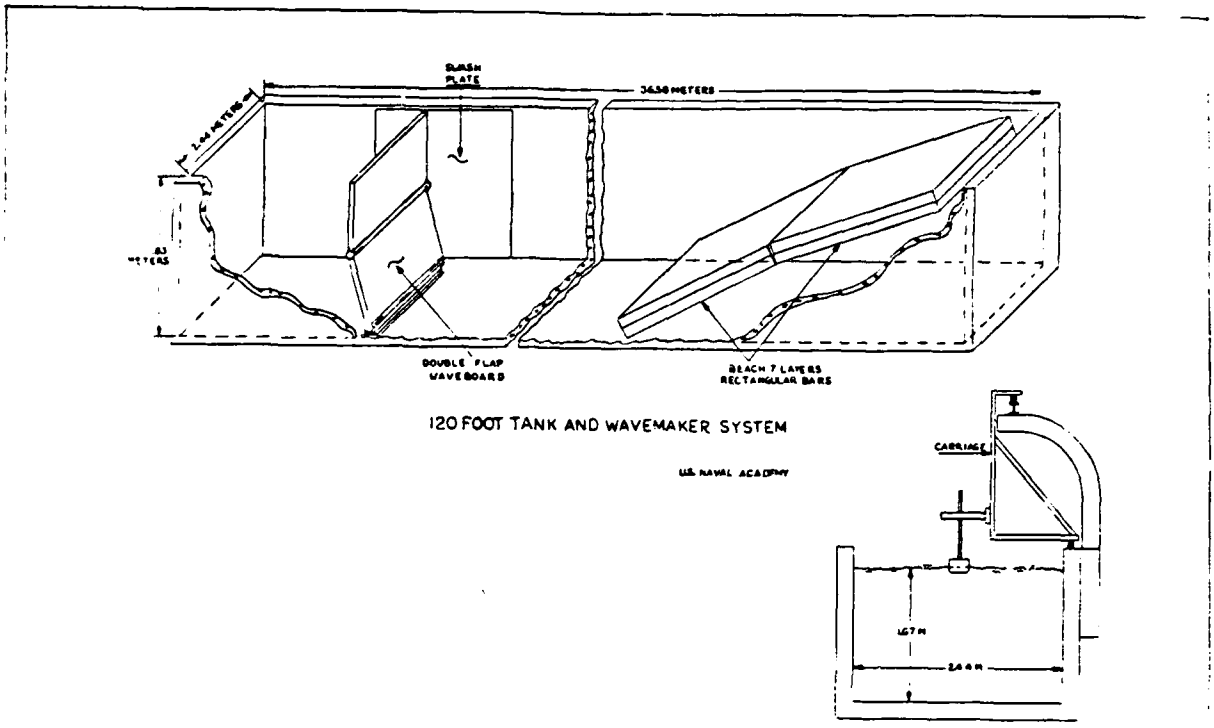

Figure 1 - U.S. Naval Academy 120 Foot Tank

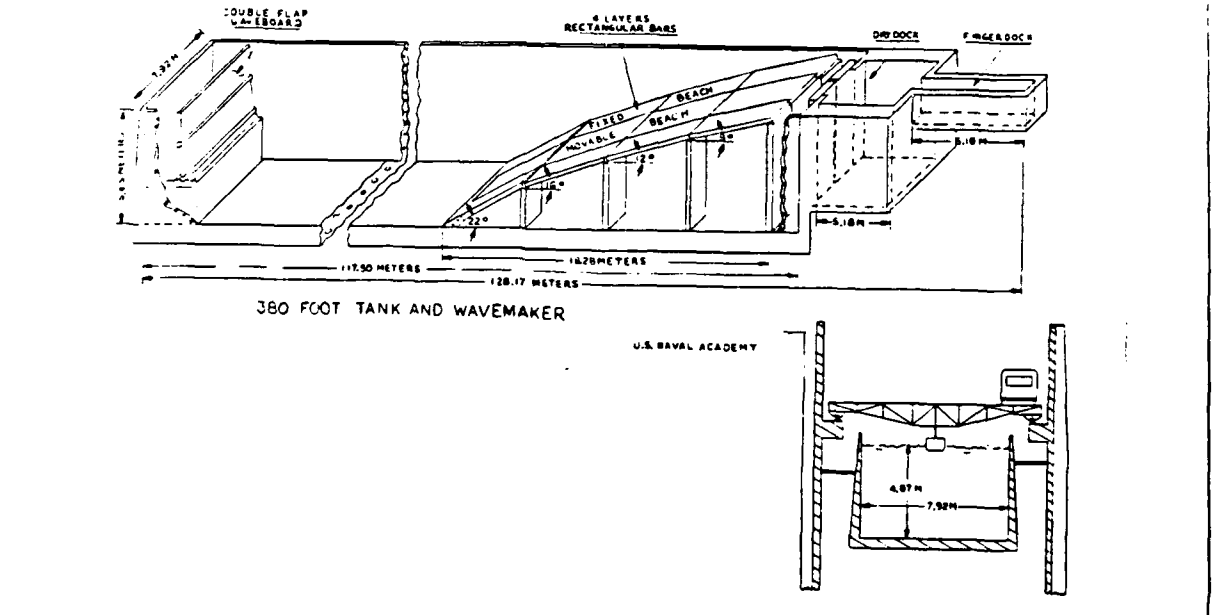

Figure 2 - U.S. Naval Academy 380 Foot Tank

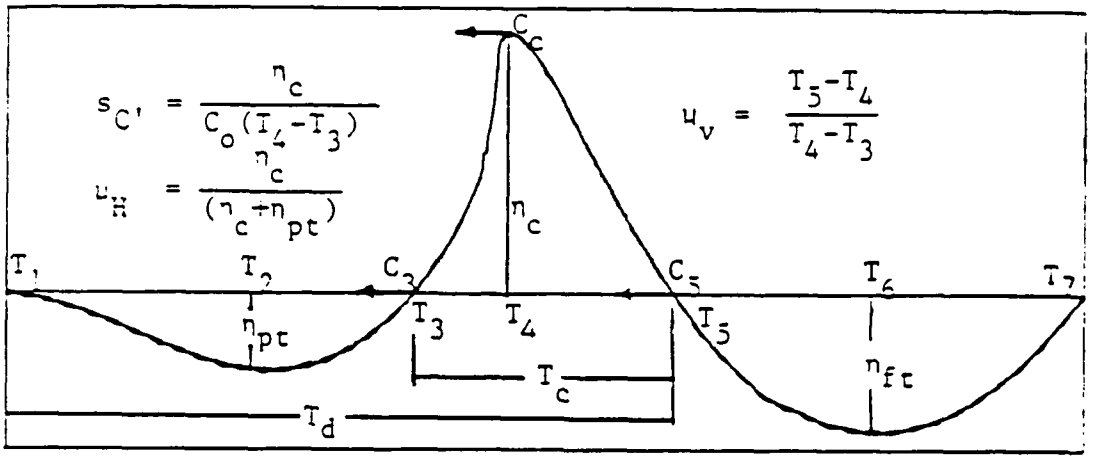

Time history of breaking wave height (from Reference 3)

C	Celerity
C_c	Crest celerity
C_o	Celerity from linear theory, $\frac{gT_d}{2\pi}$
$s_{C'}$	Crest front steepness
T	Time of probe reading
T_c	Crest period
T_d	Breaking wave period
η_c	Breaking crest amplitude
η_{ft}	Trough amplitude following breaking crest
η_{pt}	Trough amplitude preceding breaking crest
μ_H	Asymmetry about horizontal axis
μ_V	Asymmetry about vertical axis

Figure 3 - Definition of Breaking Wave Parameters from Fixed Wave Probe Time History

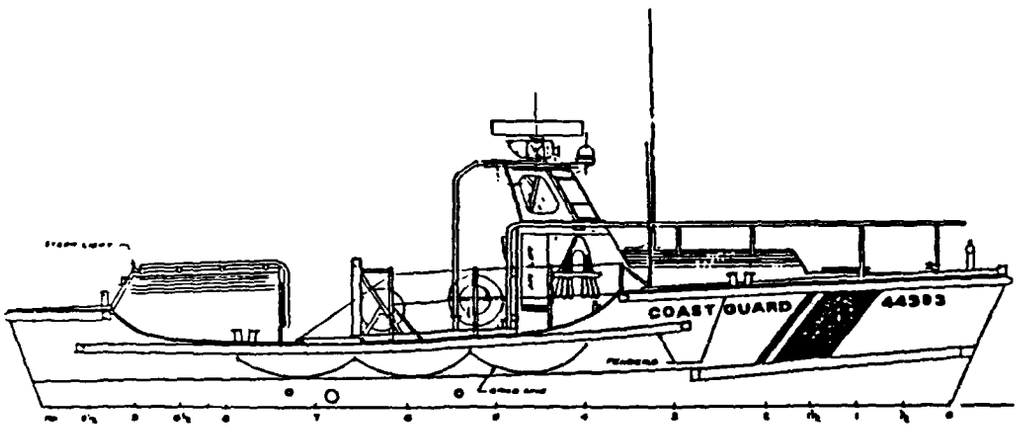

44ft MOTOR LIFEBOAT
OUTBOARD PROFILE

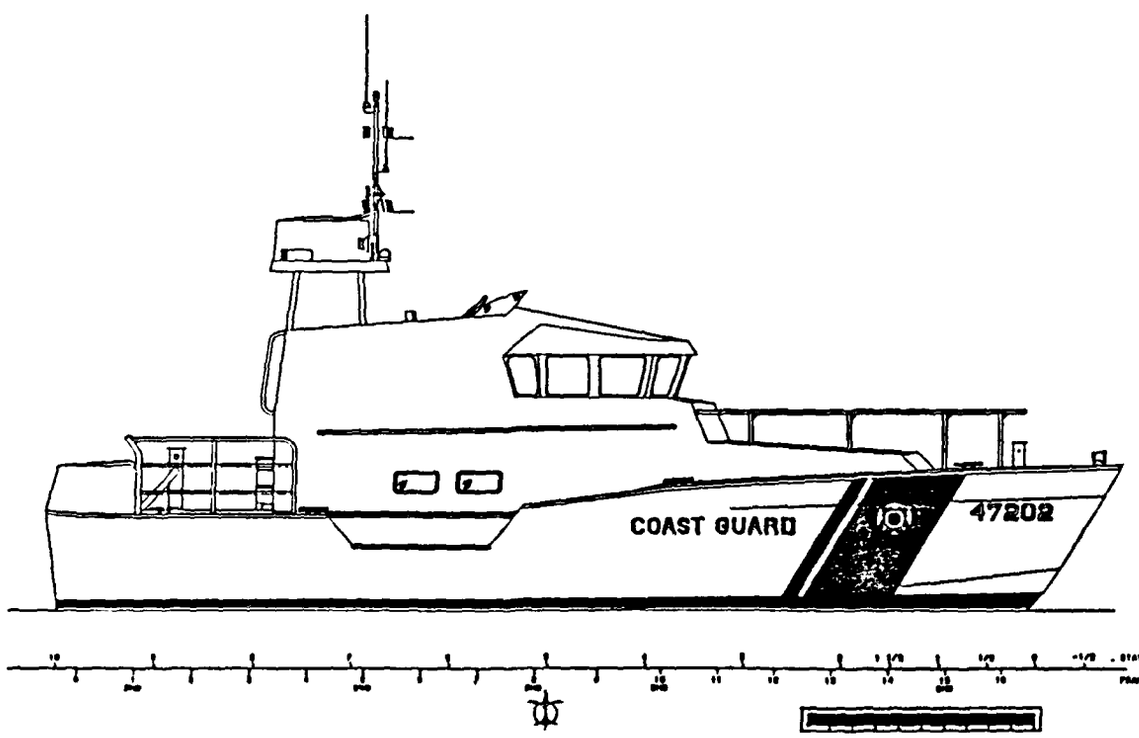

47ft CONCEPT DESIGN
OUTBOARD PROFILE

Figure 4 - Outboard Profiles of 44' and 47' Motor Lifeboats

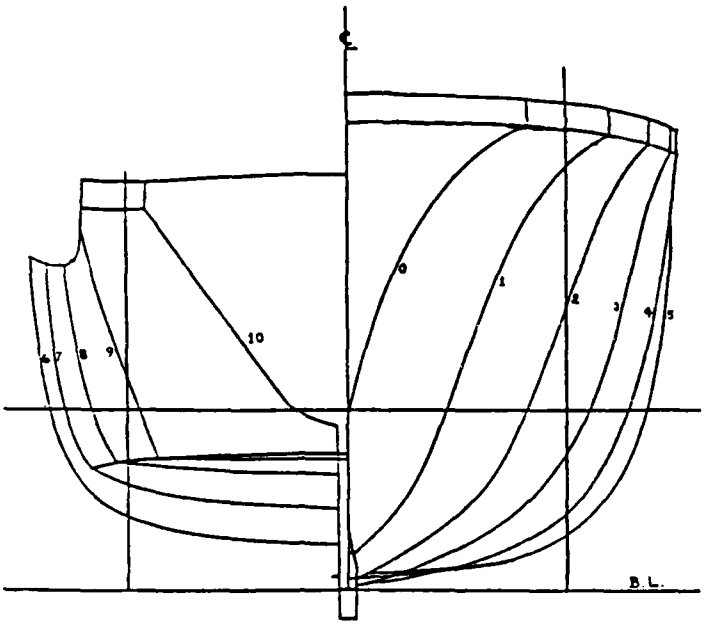

44ft MOTOR LIFEBOAT

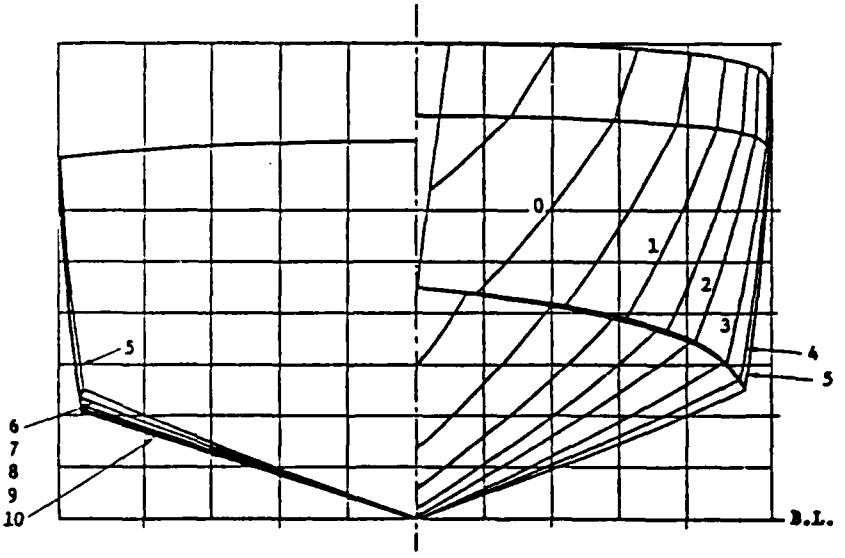

47ft CONCEPT DESIGN

Figure 5 - Body Plans of 44' and 47' Motor Lifeboats

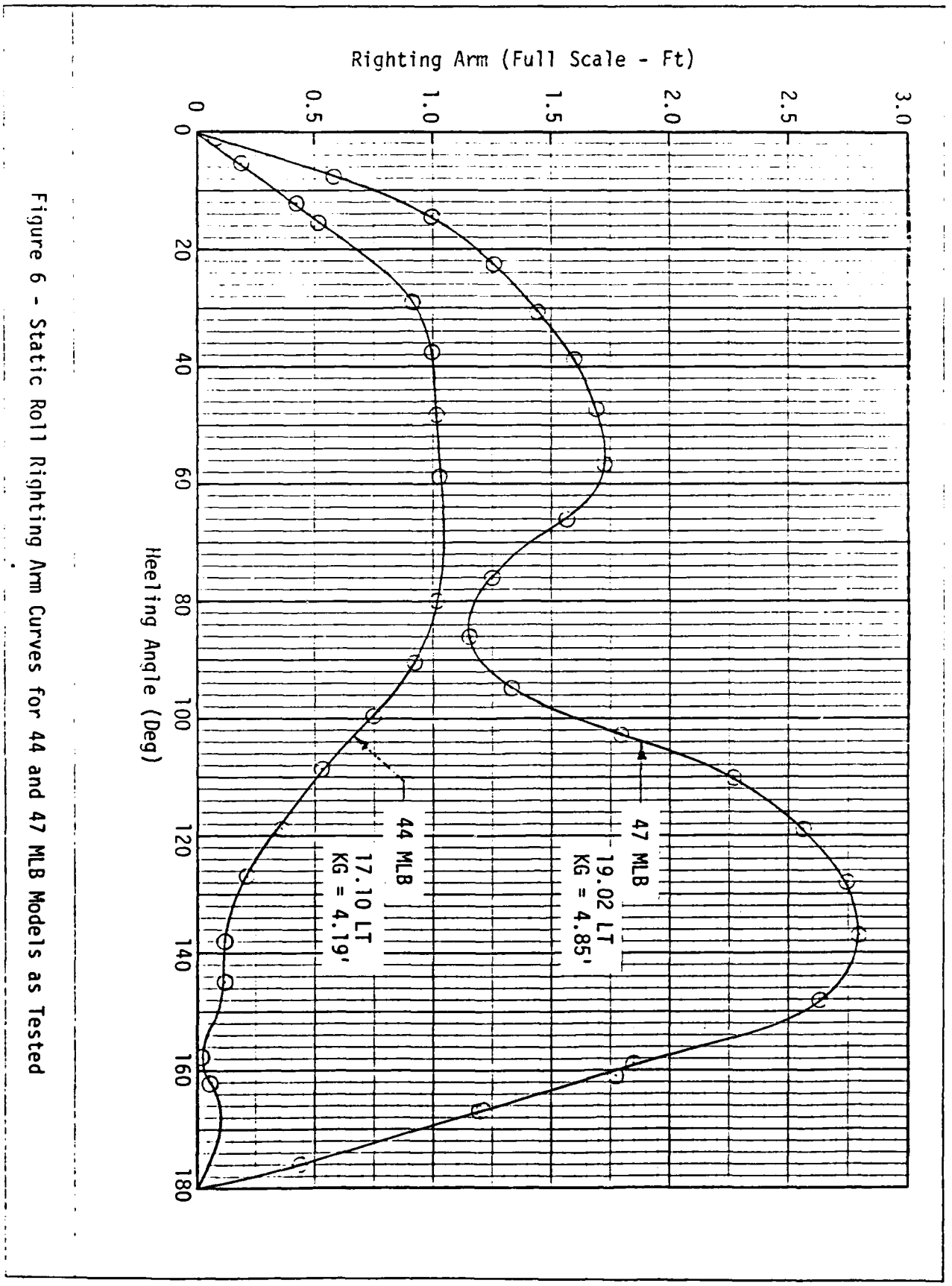

Figure 6 - Static Roll Righting Arm Curves for 44 and 47 MLB Models as Tested

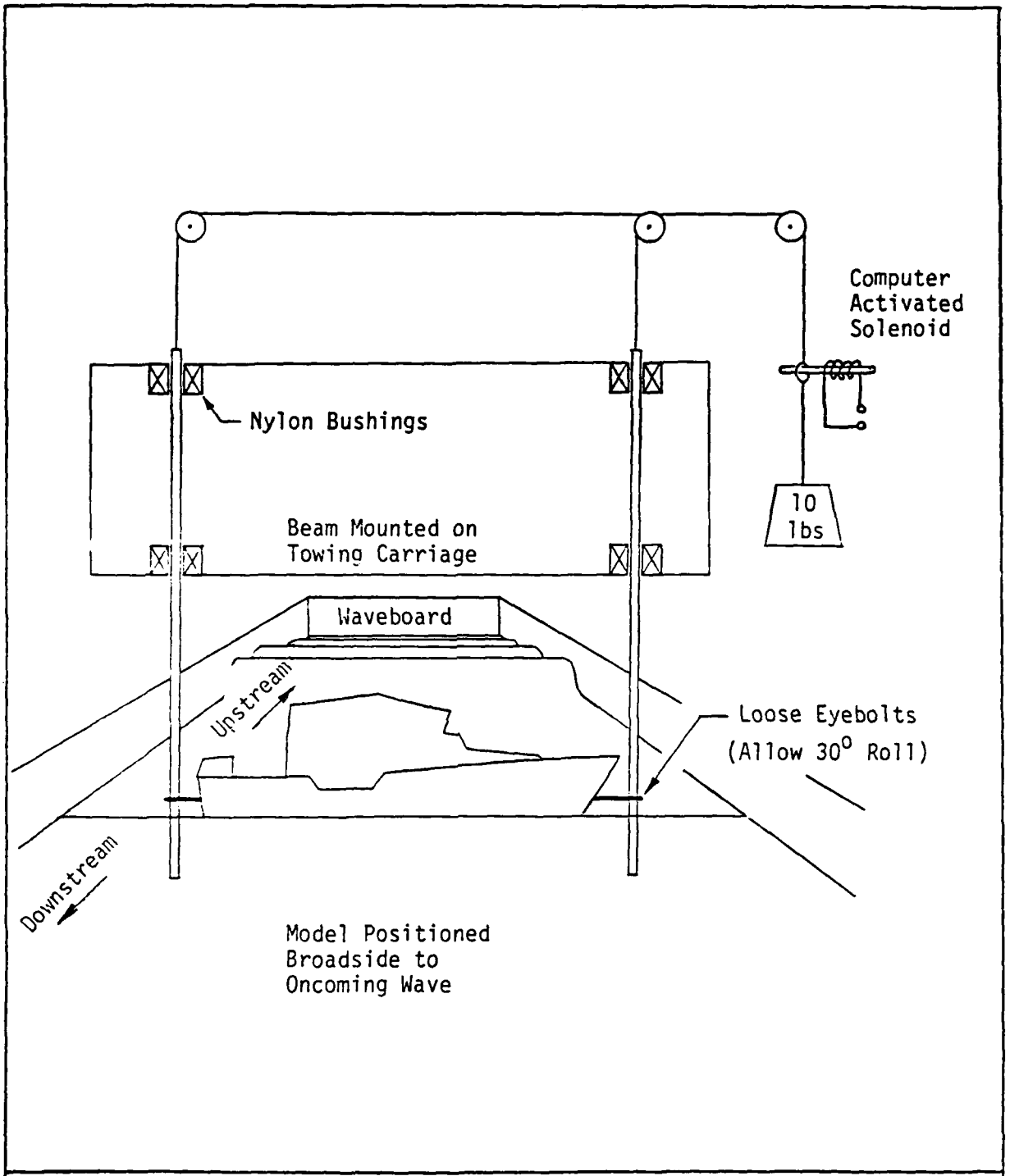

Figure 7 - Model Release Mechanism

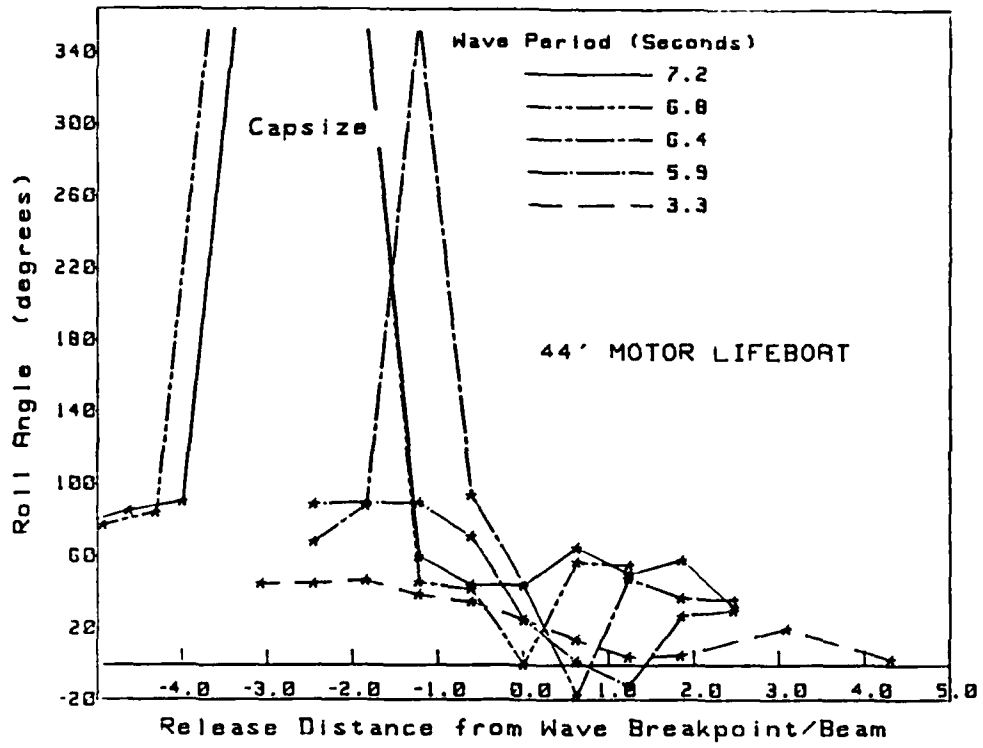

FIGURE 8a - Roll Angle vs. Nominal Breakpoint/Beam
44' MLB - Plunging Breakers

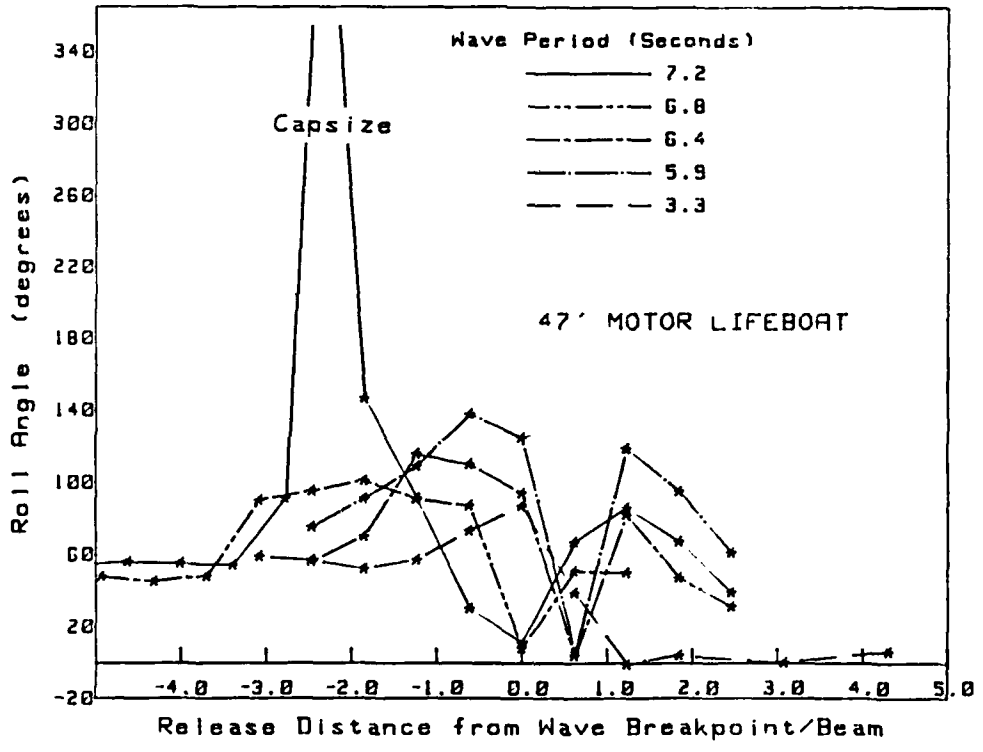

FIGURE 8b - Roll Angle vs. Nominal Breakpoint/Beam
47' MLB - Plunging Breakers

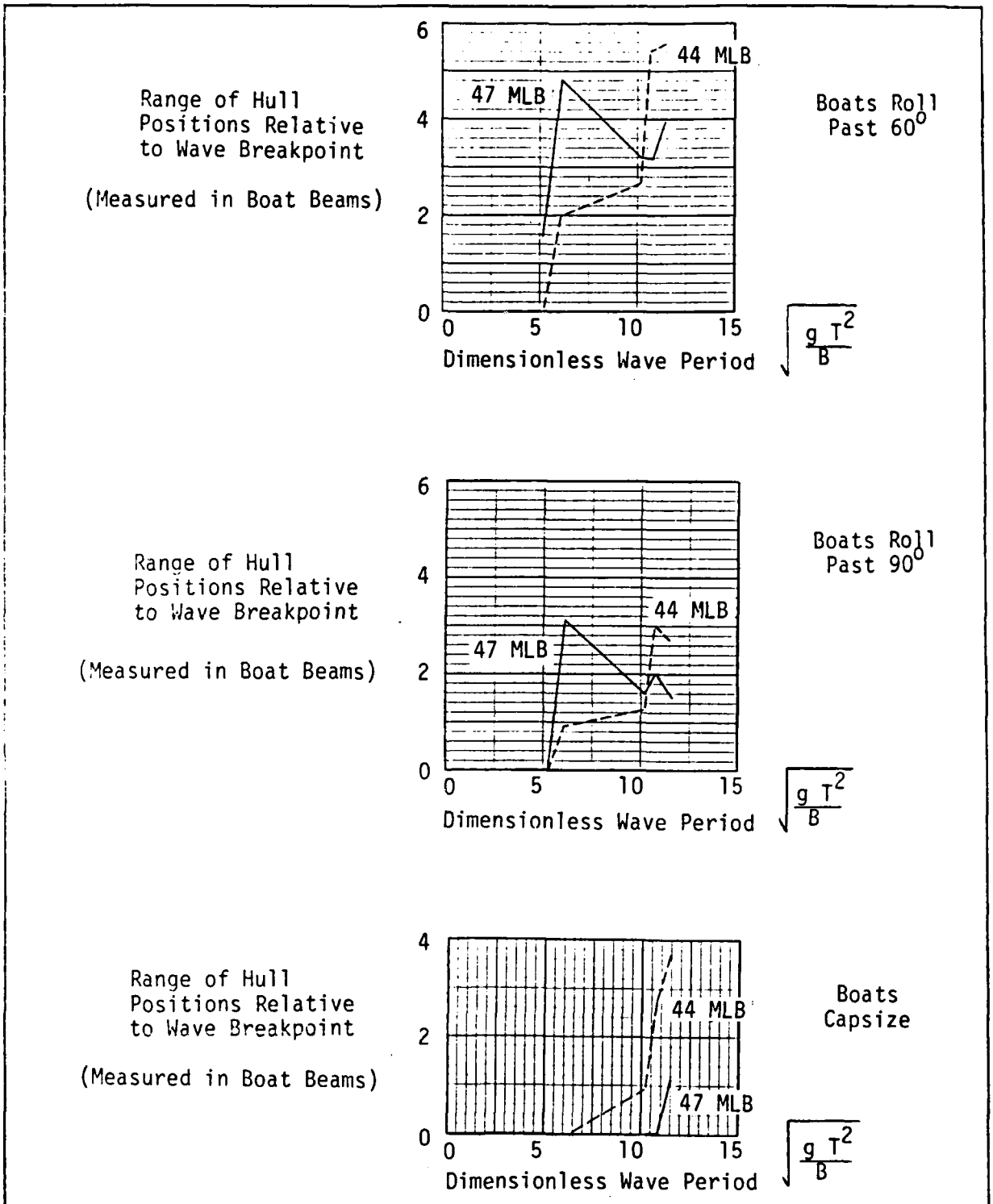

Figure 9 - Range of Hull Positions Relative to Wave Breakpoint Where Boats Roll Past Specific Angles

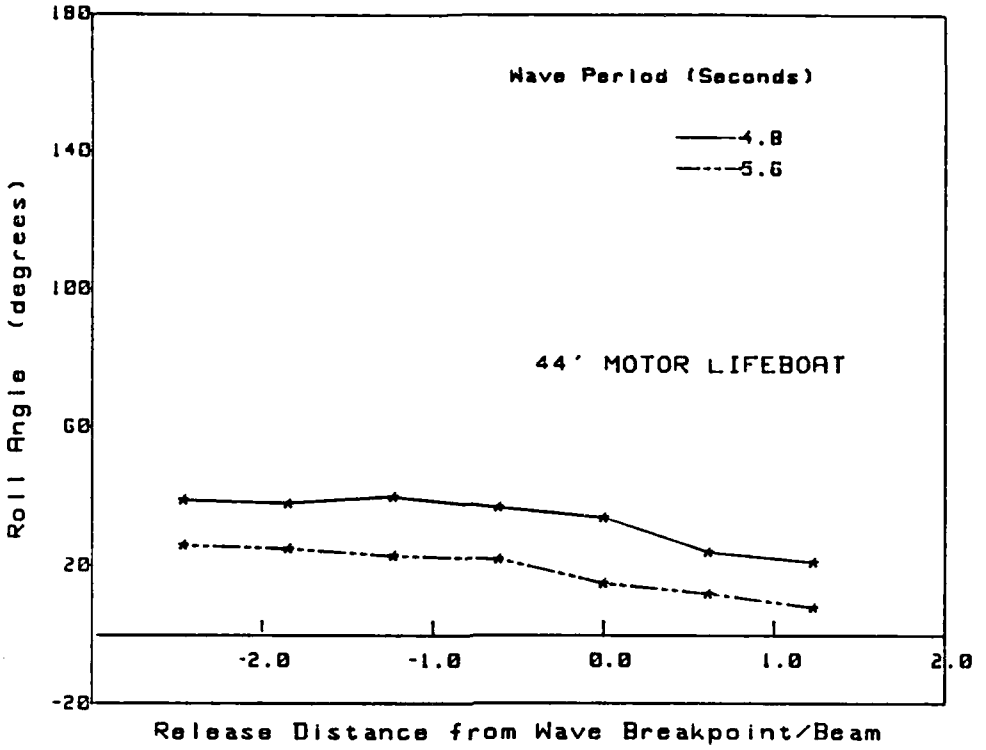

FIGURE 10a Roll Angle vs. Nominal Breakpoint/Beam
44' MLB - Spilling Breakers

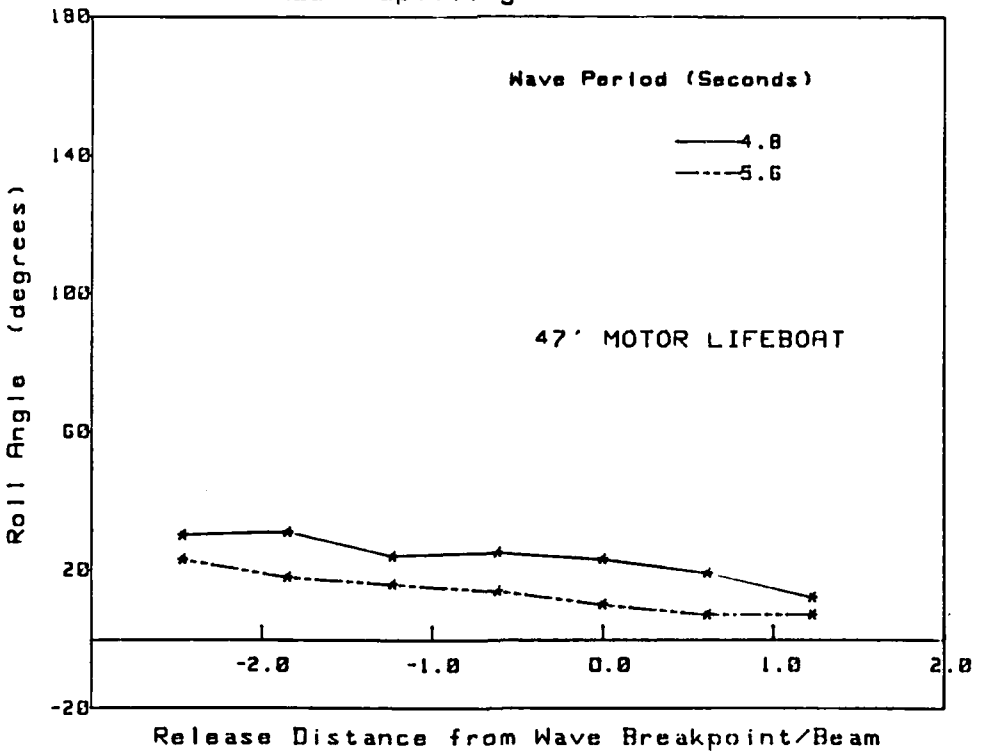

FIGURE 10b Roll Angle vs. Nominal Breakpoint/Beam
47' MLB - Spilling Breakers

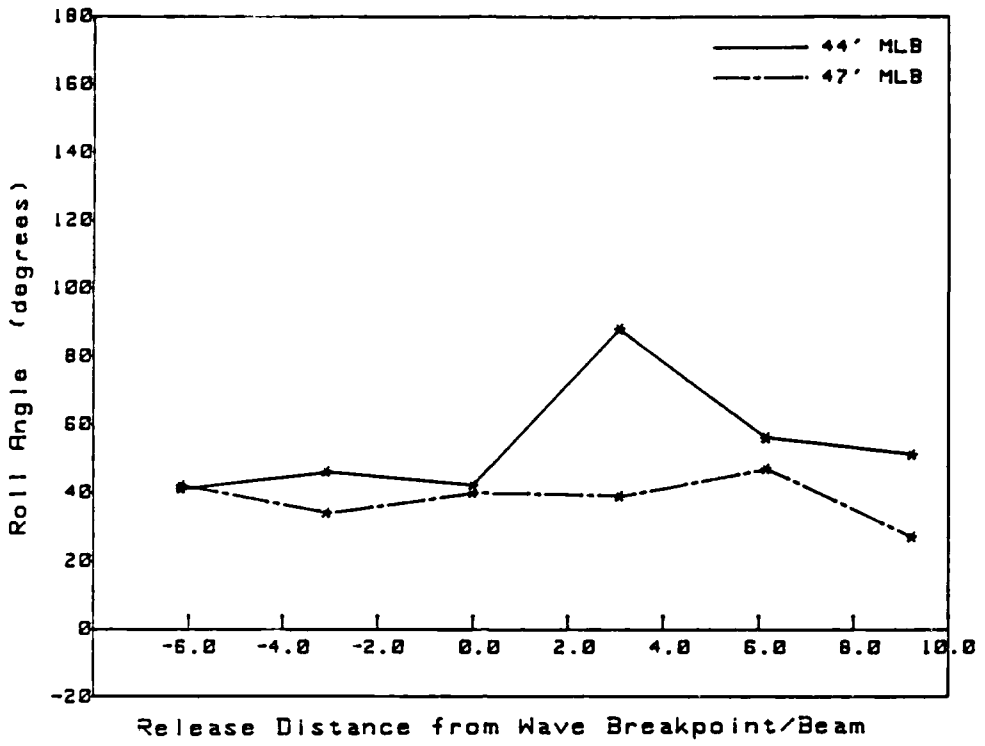

FIGURE 11 Roll Angle vs. Nominal Breakpoint/Beam
Extreme Spilling Breaker

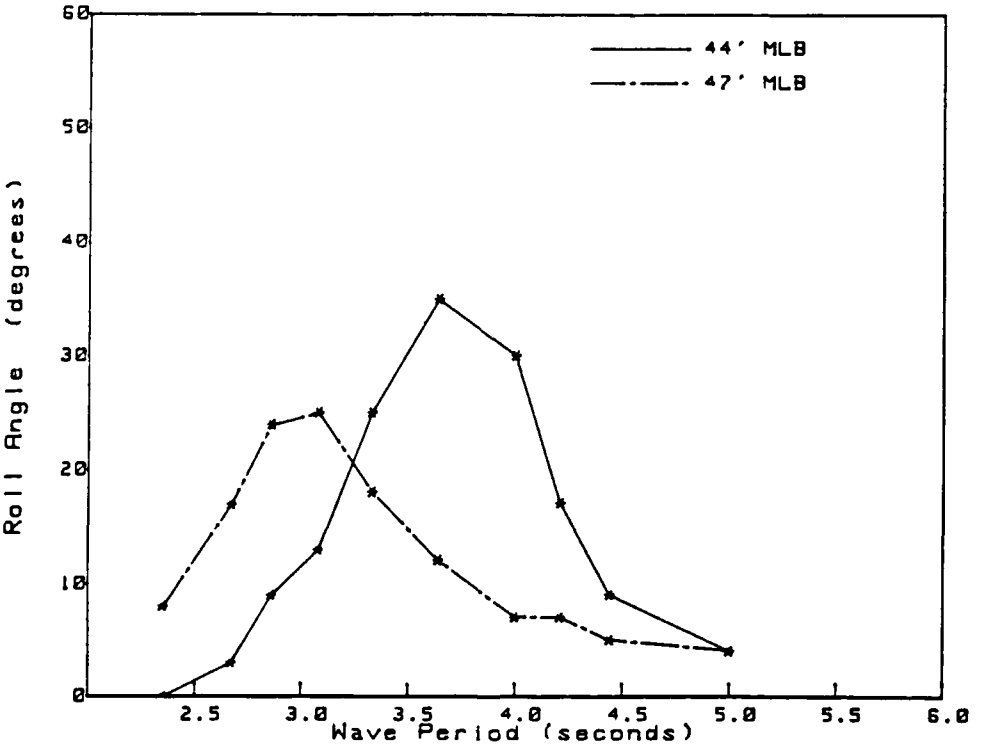

FIGURE 12 Maximum Roll Angle vs. Period of Regular Wave, H=2.7'

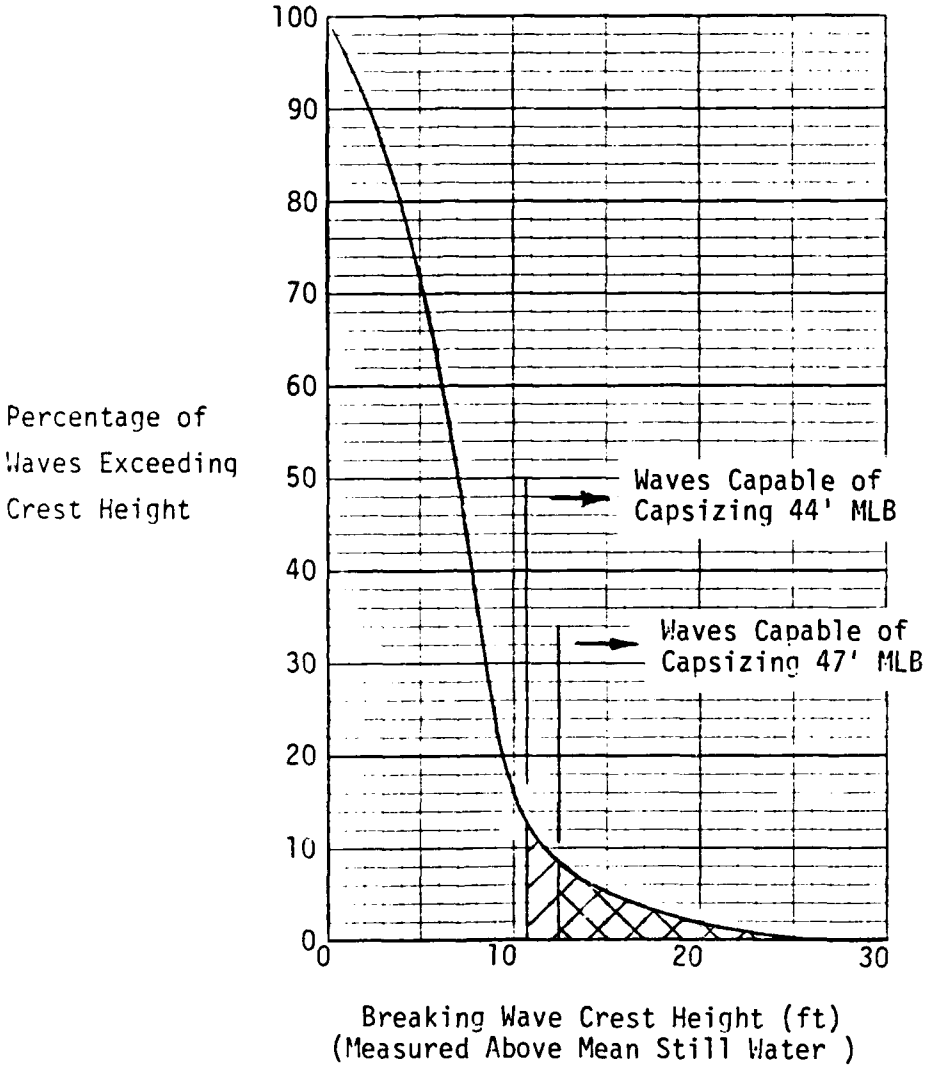

Figure 13 - Estimated Percentage of Waves at Columbia River Buoy Capable of Capsizing Motor Lifeboats